12. Mifsud A, Ramirez S, Yong EL. Androgen receptor gene CAG trinucleotide repeats in anovulatory infertility and polycystic ovaries. J Clin Endocrinol Metab 2000;85:3484–8.
13. Hickey T, Chandy A, Norman RJ. The androgen receptor CAG repeat polymorphism and X-chromosome inactivation in Australian Caucasian women with infertility related to polycystic ovary syndrome. J Clin Endocrinol Metab 2002;87:161–5.
14. Jääskeläinen J, Korhonen S, Voutilainen R, Hippeläinen M, Heinonen S. Androgen receptor gene CAG length polymorphism in women with polycystic ovary syndrome. Fertil Steril 2005;83:1724–8.
15. Allen RC, Zoghbi HY, Moseley AB, Rosenblatt HM, Belmont JW. Methylation of HpaII and HhaI sites near the polymorphic CAG repeat in the human androgen-receptor gene correlates with X chromosome inactivation. Am J Hum Genet 1992;51:1229–39.
16. Tetsuka M, Whitelaw PF, Bremner WJ, Millar MR, Smyth CD, Hillier SG. Developmental regulation of androgen receptor in rat ovary. J Endocrinol 1995;145:535–43.
17. Bachelot A, Plu-Bureau G, Thibaud E, Laborde K, Pinto G, Samara D, et al. Long-term outcome of patients with congenital adrenal hyperplasia due to 21-hydroxylase deficiency. Horm Res 2006;67:268–76.
18. Migeon BR, Jelalian K. Evidence for two active X chromosomes in germ cells of female before meiotic entry. Nature 1977;269:242–3.
19. Sharp A, Robinson D, Jacobs P. Age- and tissue-specific variation of X chromosome inactivation ratios in normal women. Hum Genet 2000;107:343–9.
20. Shiina H, Matsumoto T, Sato T, Igarashi K, Miyamoto J, Takemasa S, et al. Premature ovarian failure in androgen receptor-deficient mice. Proc Natl Acad Sci U S A 2005;103:224–9.

RESEARCH LETTER

AMERICAN JOURNAL OF medical genetics

Mutation Analysis of *SOX9* and Single Copy Number Variant Analysis of the Upstream Region in Eight Patients With Campomelic Dysplasia and Acampomelic Campomelic Dysplasia

Yuka Wada,[1]* Gen Nishimura,[2] Toshiro Nagai,[3] Hideaki Sawai,[4] Mayumi Yoshikata,[5] Shinichirou Miyagawa,[6] Takushi Hanita,[7] Seiji Sato,[8] Tomonobu Hasegawa,[9] Shumpei Ishikawa,[10] and Tsutomu Ogata[1]

[1]Department of Endocrinology and Metabolism, National Research Institute for Child Health and Development, Tokyo, Japan

[2]Department of Radiology, Tokyo Metropolitan Kiyose Children's Hospital, Kiyose, Japan

[3]Department of Pediatrics, Dokkyo Medical University, Koshigaya, Japan

[4]Genetic Counseling and Clinical Research Unit, Kyoto University, Kyoto, Japan

[5]Department of Neonatology, Hyogo Children's Hospital, Kobe, Japan

[6]Department of Pediatrics, National Hospital Organization Kure Medical Center, Kure, Japan

[7]Department of Pediatrics, Tohoku University School of Medicine, Sendai, Japan

[8]Department of Pediatrics, Saitama City Hospital, Saitama, Japan

[9]Department of Pediatrics, School of Medicine, Keio University, Tokyo, Japan

[10]Genome Science Division, Department of Pathology, Research Center for Advanced Science and Technology, Graduate School of Medicine, University of Tokyo, Tokyo, Japan

Received 21 August 2009; Accepted 16 July 2009

TO THE EDITOR:

Campomelic dysplasia (CD; OMIM 114290) is a rare skeletal disorder characterized by hypoplastic scapulae, 11 pairs of ribs, pelvic abnormalities, and bowing of the lower limb bones [Maroteaux et al., 1971]. Affected patients often die shortly after birth due to respiratory distress, and roughly two-thirds of affected genetic males have disorders of sex development (DSD) due to dysgenetic testes [Mansour et al., 1995]. Acampomelic campomelic dysplasia (ACD) is associated with similar but milder skeletal features and lacks long bone curvature [MacPherson et al., 1989].

SOX9 on chromosome 17q24 is a member of SRY-related gene family [Harley et al., 2003]. It encodes a 509-amino acid protein that harbors a high mobility group (HMG) domain with a DNA-binding capacity and a proline/glutamine/serine-rich domain with a transactivation function [Harley et al., 2003]. Furthermore, putative *cis*-control elements have been mapped within the 1 Mb region upstream of *SOX9* [Hill-Harfe et al., 2005].

To date, it has been shown that both CD and ACD can be caused by heterozygous intragenic *SOX9* mutations or chromosomal aberrations (translocations, inversions, or deletions) affecting *SOX9* or the putative enhancer region [Pfeifer et al., 1999; Thong et al., 2000; Moog et al., 2001; Harley et al., 2003; Pop et al., 2004; Leipoldt et al., 2007]. However, the frequency and the type of mutations and chromosomal aberrations are quite different

How to Cite this Article:
Wada Y, Nishimura G, Nagai T, Sawai H, Yoshikata M, Miyagawa S, Hanita T, Sato S, Hasegawa T, Ishikawa S, Ogata T. 2009. Mutation analysis of *SOX9* and single copy number variant analysis of the upstream region in eight patients with campomelic dysplasia and acampomelic campomelic dysplasia.
Am J Med Genet Part A 149A:2882–2885.

*Correspondence to:
Yuka Wada, M.D., Department of Endocrinology and Metabolism, National Research Institute for Child Health and Development, 2-10-1 Ohkura, Setagaya, Tokyo 157-8535, Japan. E-mail: ywada@nch.go.jp
Published online 16 November 2009 in Wiley InterScience (www.interscience.wiley.com)
DOI 10.1002/ajmg.a.33107

TABLE I. Clinical and Molecular Findings in Patients Examined in This Study

	Campomelic dysplasia				Acampomelic campomelic dysplasia			
	Patient 1	Patient 2	Patient 3	Patient 4	Patient 5	Patient 6	Patient 7	Patient 8
Patient								
Gastational age (weeks)	25	42	38	38	39	40	42	38
Birth weight (g)	625	2490	2670	2060	3400	2700	2680	2306
Present age (y:m)	Stillbirth	0:11	(0:5)[a]	(1:5)[a]	11:6	19:8	3:2	3:9
Karyotype	46,XY	46,XX	46,XX	46,XX	46,XY	46,XY	46,XX	46,XX
Phenotype								
Cleft palate	−	−	+	−	+	+	+	+
Micrognathia	+	+	+	+	+	−	−	+
Scapular hypoplasia	+	+	+	+	+	+	+	+
Tibial bowing	+	+	+	+	−	−	−	−
Femoral bowing	+	+	+	+	−	−	−	−
11 pairs of ribs	−	+	+	+	−	+	+	+
Small thoracic cage	+	+	+	+	+	+	+	−
NM thoracic pedicles	+	+	+	+	−	−	+	+
Scoliosis	−	−	−	−	+	+	+	−
Narrow iliac wings	±	+	+	+	±	±	±	+
Clubfeet	+	+	+	+	−	−	−	+
46,XY DSD	+	−	−	−	−	−	−	−
Mutation								
cDNA	771_772insGGCGC	1330_1333delGACC	T338C	G442T	C509T	−	−	−
Amino acids	G257fsX296	T443fsX468	M113T	E148X	P170L	−	−	−

NM: non-mineralized; DSD: disorders of sex development.
[a]Deceased at 5 months and 1 year and 5 months, respectively.

between CD and ACD. CD is predominantly caused by nonsense or frameshift mutations or by chromosomal aberrations disrupting *SOX9*, although missense mutations and chromosomal aberrations impairing the enhancer region are also occasionally identified. By contrast, ACD is almost exclusively caused by missense mutations or by chromosomal aberrations affecting the enhancer region. Thus, while missense mutations are exclusively identified within the HMG box in both CD and ACD [Kwok et al., 1995; Cameron and Sinclair, 1997; Meyer et al., 1997; Hageman et al., 1998; Moog et al., 2001; Thong et al., 2000], these findings imply that severe mutations usually result in CD whereas mild mutations usually lead to ACD.

However, the underlying causes remain to be determined in several patients, especially those with ACD, and such patients may have hidden perturbation in the putative enhancer region. Thus, we performed mutation analysis of *SOX9* in eight patients with CD or ACD and single copy number variant (CNV) analysis [Redon et al., 2006] of the upstream region in *SOX9* mutation negative patients.

Clinical features of the eight patients are summarized in Table I, and representative roentgenograms are shown in Figure 1. Patients 1–4 showed CD-compatible severe clinical features, whereas patients 5–8 exhibited relatively mild ACD-compatible clinical features. In addition, patient 1 ended in a stillbirth, and patients 3 and 4 died of respiratory insufficiency during infancy, although patient 2 aged 11 months was alive. By contrast, patients 5–8 have survived a relatively long period. Among genetic males, patient 1 exhibited DSD with nearly complete female external genitalia, while patients 5 and 6 showed male external genitalia.

We first performed mutation analysis of *SOX9*. This study was approved by the Institutional Review Board Committees at National Center for Child Health and Development, and performed after obtaining written informed consent. Genomic DNA samples

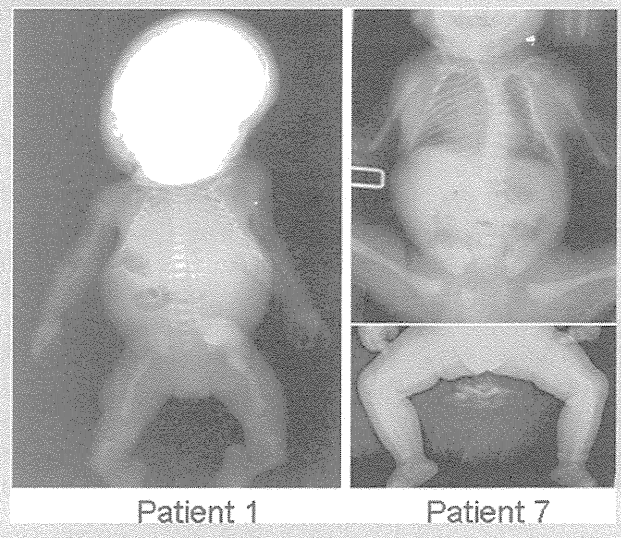

FIG. 1. Representative roentgenograms indicating CD in patient 1 at birth and ACD in patient 7 at 3 months of age.

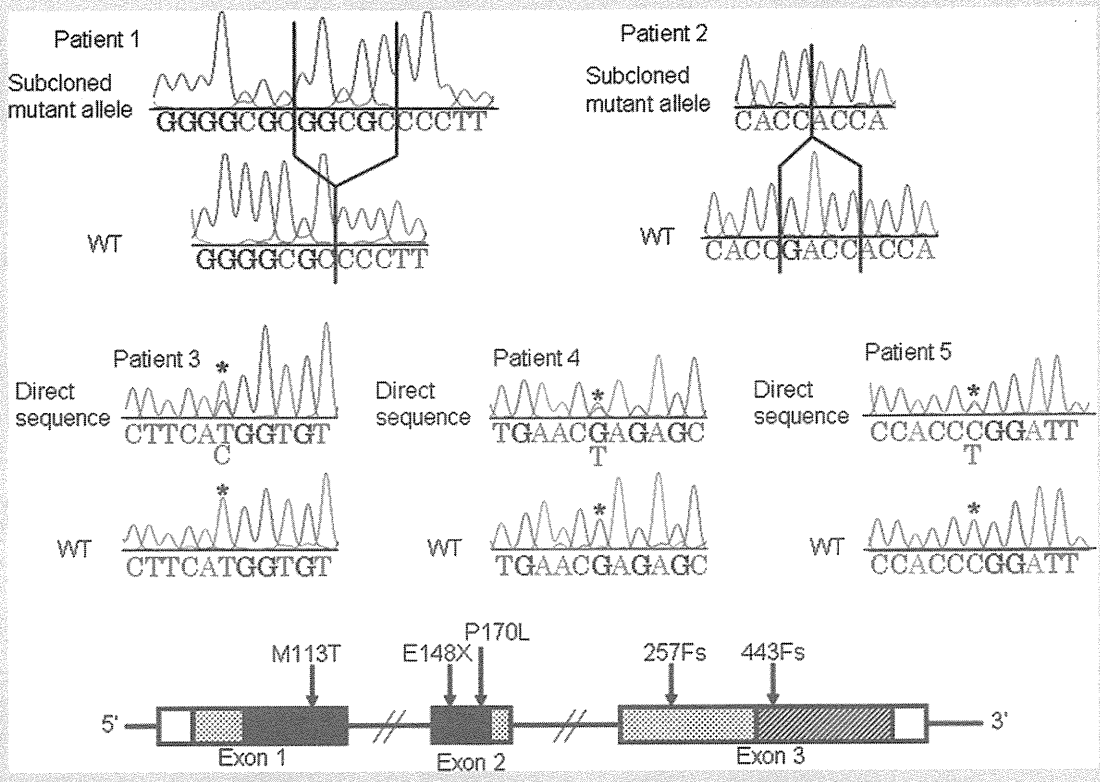

FIG. 2. Molecular findings in patients 1–5 with *SOX9* mutations. Upper part: Electrochromatograms showing the mutations in patients 1–5. In patients 1 and 2, the subcloned mutant alleles and the corresponding wildtype (WT) alleles are shown. In patients 3–5, the direct sequences are shown, together with the corresponding wildtype sequences; the asterisks indicate the mutant and the corresponding wildtype nucleotides. Lower part: The position of the mutations on the genomic sequences. Exons 1–3 are depicted with boxes; the black, the striped, the stippled, and the white areas indicate the HMG domain, the transactivation domain, other translated regions, and the untranslated regions, respectively.

extracted from cord blood cells (patient 1) or peripheral blood cells (patients 2–8) were amplified by PCR for all the three coding exons and were subjected to direct sequencing on a CEQ 8000 autosequencer (Beckman Coulter, Fullerton, CA) (the primer sequences are available on request). To confirm frameshift mutations, the corresponding PCR products were subcloned with TOPO TA Cloning Kit (Invitrogen, Carlsbad, CA) and normal and mutant alleles were sequenced separately.

Consequently, we identified a novel heterozygous 5-bp insertion mutation at exon 3 that is predicted to cause a frameshift at the 257th glycine codon and resultant termination at the 296th codon (G257fsX296) in patient 1, a novel heterozygous 4-bp deletion mutation at exon 3 that is predicted to cause a frameshift at the 443rd threonine codon and resultant termination at the 468th codon (T443fsX468) in patient 2, a novel heterozygous missense mutation at exon 1 (M113T) in patient 3, a recurrent heterozygous nonsense mutation at exon 2 (E148X) in patient 4, and a novel heterozygous missense mutation at exon 2 (P170L) in patient 5 (Fig. 2). The two missense mutations resided within the HMG. The mutations of patients 1–4 were absent in their parents. In addition, while mutation analysis was refused by the parents of patient 5, the P170L missense mutation was absent in 200 control subjects. No mutations were identified in patients 6–8.

Then, to examine for a small deletion, we carried out the whole genome CNV analysis in patients 6–8 and their parents, using custom high density oligonucleotide microarray based on Affymetrix platform [Redon et al., 2006]. In brief, 25 bp oligonucleotide probes are designed on 1,330,354 *Nsp* I restriction fragments with average and median spacing of 2,271 and 776 bp. The experimental protocol is the same as the Affymetrix 500K arrays. Ninety microgram of target was hybridized overnight to the arrays [Fujii et al., 2007]. The signal intensity ratio of the sample to reference was calculated by Genome Imbalance Map Algorithm [Ishikawa et al., 2005], using NA10851 HapMap DNA samples from Coriell Cell Repositories (Camden, NJ) as the reference samples. Consequently, no deletion was indicated in the whole genome including the 5′ region of *SOX9* in patients 6–8.

The results are primarily consistent with the previous data. Three of four patients with CD died during fetal life or infancy, whereas patients 5–8 with ACD survived into childhood or puberty. 46,XY with DSD was observed in patient 1 with CD but not in patients 5 and 6 with ACD. Similarly, truncating mutations of *SOX9* were identified in patients 1–3 with CD, together with a missense mutation in patient 4 with CD, whereas only one missense mutation was found in patients with ACD.

We could not detect a microdeletion in patients 6–8 with ACD in whom no intragenic mutations were identified. Although the underlying causes remain to be clarified in patients 6–8, there are several possible explanations for the development of ACD in patients 6–8. First, a mutation(s) may exist in the unexamined intronic or the downstream region. Second, a tiny deletion may remain undetected. Third, there may be a mutation in some gene(s) other than *SOX9*. Further studies will identify underlying mechanisms involved in the development of ACD in *SOX9* mutation negative patients.

REFERENCES

Cameron FJ, Sinclair AH. 1997. Mutation in SRY and SO X9: Testis-determining genes. Hum Mutat 9:388–395.

Fujii K, Ishikawa S, Uchikawa H, Komura D, Shapero MH, Shen F, Hung J, Arai H, Tanaka Y, Sasaki K, Kohno Y, Yamada M, Jones KW, Aburatani H, Miyashita T. 2007. High-density oligonucleotide array with sub-kilobase resolution reveals breakpoint information of submicroscopic deletions in nevoid basal cell carcinoma syndrome. Hum Genet 122:459–466.

Hageman RM, Cameron FJ, Sinclair AH. 1998. Mutation analysis of the SOX9 gene in a patient with campomelic dysplasia. Hum Mutat Suppl 1:S112–S113.

Harley VR, Clarkson MJ, Argentaro A. 2003. The molecular action and regulation of the testis-determining factors, SRY (sex-determining region on the Y chromosome) and SOX9 [SRY-related high-mobility group (HMG) box 9]. Endocr Rev 24:466–487.

Hill-Harfe KL, Kaplan L, Stalker HJ, Zori RT, Pop R, Scherer G, Wallace MR. 2005. Fine mapping of chromosome 17 translocation breakpoints >900 kb upstream of *SOX9* in acampomelic campomelic dysplasia and a mild, familial skeletal dysplasia. Am J Hum Genet 76:663–671.

Ishikawa S, Komura D, Tsuji S, Nishimura K, Yamamoto S, Panda B, Huang J, Fukayama M, Jones KW, Aburatani H. 2005. Allelic dosage analysis with genotyping microarrays. Biochem Biophys Res Commun 333:1309–1314.

Kwok C, Weller PA, Guioli S, Foster JW, Mansour S, Zuffardi O, Punnett HH, Dominguez-Steglich MA, Brook JD, Young ID, Goodfellow PN, Schafer AJ. 1995. Mutations in SOX9, the gene responsible for Campomelic dysplasia and autosomal sex reversal. Am J Hum Genet 57: 1028–1036.

Leipoldt M, Erdel M, Bien-Willner GA, Smyk M, Theurl M, Yatsenko SA, Lupski JR, Lane AH, Shanske AL, Stankiewicz P, Schere G. 2007. Two novel translocation breakpoints upstream of SOX9 define borders of the proximal and distal breakpoint cluster region in campomelic dysplasia. Clin Genet 71:67–75.

MacPherson RI, Skinner SA, Donnenfeld AE. 1989. Acampomelic campomelic dysplasia. Pediatr Radiol 20:90–93.

Mansour S, Hall CM, Pembery ME, Young ID. 1995. A clinical and genetic study of campomelic dysplasia. J Med Genet 32:145–420.

Maroteaux P, Spranger J, Opitz J, Kucera J, Lowry R, Schimke R, Kagan S. 1971. Le syndrome campomelique. Presse Med 22:1157–1162.

Meyer J, Südbeck P, Held M, Wagner T, Schmitz ML, Bricarelli FD, Eggermont E, Friedrich U, Haas OA, Kobelt A, Leroy JG, Van Maldergem L, Michel E, Mitulla B, Pfeiffer RA, Schinzel A, Schmidt H, Scherer G. 1997. Mutational analysis of the SOX9 gene in campomelic dysplasia and autosomal sex reversal: Lack of genotype/phenotype correlations. Hum Mol Genet 6:91–98.

Moog U, Jansen NJ, Scherer G, Schrander-Stumpel CT. 2001. Acampomelic campomelic syndrome. Am J Med Genet 104:239–245.

Pfeifer D, Kist R, Dewar K, Devon K, Lander ES, Brirren B, Korniszewski L, Back E, Scherer G. 1999. Campomelic dysplasia translocation breakpoints are scattered over 1 Mb proximal to *SO* X9: Evidence for an extended control region. Am J Hum Genet 65:111–124.

Pop R, Conz C, Lindenberg KS, Blesson S, Schmalenberger B, Briault S, Pfeifer D, Scherer G. 2004. Screening of the 1 Mb SOX9 5' control region by array CGH identifies a large deletion in a case of campomelic dysplasia with XY sex reversal. J Med Genet 41:e47.

Redon R, Ishikawa S, Fitch KR, Feuk L, Perry GH, Andrews TD, Fiegler H, Shapero MH, Carson AR, Chen W, Cho EK, Dallaire S, Freeman JL, González JR, Gratacòs M, Huang J, Kalaitzopoulos D, Komura D, MacDonald JR, Marshall CR, Mei R, Montgomery L, Nishimura K, Okamura K, Shen F, Somerville MJ, Tchinda J, Valsesia A, Woodwark C, Yang F, Zhang J, Zerjal T, Zhang J, Armengol L, Conrad DF, Estivill X, Tyler-Smith C, Carter NP, Aburatani H, Lee C, Jones KW, Scherer SW, Hurles ME. 2006. Global variation in copy number in the human genome. Nature 444:444–454.

Thong MK, Scherer G, Kozlowski K, Haan E, Morris L. 2000. Acampomelic campomelic dysplasia with SOX9 mutation. Am J Med Genet 93: 421–425.

European Journal of Endocrinology (2009) 161 301–306 ISSN 0804-4643

CLINICAL STUDY

An immunologically anomalous but considerably bioactive GH produced by a novel *GH1* mutation (p.D116E)

Sumito Dateki, Kazuko Hizukuri[1], Toshiaki Tanaka[2], Noriyuki Katsumata, Paravee Katavetin and Tsutomu Ogata

Department of Endocrinology and Metabolism, National Research Institute for Child Health and Development, 2-10-1 Ohkura, Setagaya, Tokyo 157-8535, Japan, [1]Department of Pediatrics, Kagoshima University School of Medicine, Kagoshima 890-8544, Japan and [2]Tanaka Growth Clinic, Tokyo 154-0004, Japan

(Correspondence should be addressed to T Ogata; Email: tomogata@nch.go.jp)

Abstract

Contex: Although GH values measured by an immunoassay usually reflect GH bioactivities, discrepancy exists between immunoactivity and bioactivity in a rare condition known as 'bioinactive GH'.
Objective: To report an immunologically anomalous but considerably bioactive GH.
Methods: We performed mutational and functional analyses of *GH1* in a 7-year-old Japanese boy with short stature (−3.0 S.D.) in whom serum GH values measured with a Tosoh immunoassay kit were all undetectable in three provocation tests, whereas urine GH value measured with a Hitachi immunoassay kit was within the normal range. Serum IGF-1 was at a low-normal range, and IGF-binding protein-3 was below the normal range.
Results: Mutation analysis showed a missense GH produced by a novel *GH1* mutation (p.D116E) of paternal origin and a frameshift mutation (p.Q68fsX106) of maternal origin. Genotype–phenotype correlations in this family and *in vitro* functional studies indicated that the p.D116E-GH was immeasurable with the Tosoh kit but was measurable, though maybe not precise, with a Daiichi kit, and had a reduced *in vivo* bioactivity. The p.Q68fsX106 yielded no GH protein.
Conclusions: The results suggest that the p.D116E affects the GH epitope primarily recognized by the Tosoh kit but not by the Hitachi or the Daiichi kits, thereby producing an immunologically anomalous but considerably bioactive GH. The presence of such a hormone discordant for immunoactivity and bioactivity should be kept in mind, to allow for an appropriate assessment of endocrine data.

European Journal of Endocrinology **161** 301–306

Introduction

GH measurement by an immunoassay is indispensable for the diagnosis of GH deficiency. Indeed, GH provocation tests are almost invariably performed in children with short stature (1), and measured serum GH values usually reflect GH bioactivities. However, in a rare condition known as 'bioinactive GH', discrepancy exists between measured GH values and GH bioactivities (2–4). Thus, this condition is associated with low insulin-like growth factor-1 (IGF-1) values, short stature, and good responses to GH therapy, in the presence of apparently normal to mildly elevated serum GH values.

Here, we report an immunologically anomalous but considerably bioactive GH identified in a patient with short stature.

Patient and methods

Case report

This Japanese boy was born to non-consanguineous parents at 39 weeks of gestation after an uncomplicated pregnancy and delivery. At birth, his length was 50.0 cm (+0.6 S.D.) and his weight was 2.97 kg (+0.2 S.D).

At 7 years and 1 month of age, he was referred to us because of proportionate short stature (Fig. 1). Endocrine and auxological data are summarized in Tables 1 and 2. Notably, serum GH values measured with a Tosoh immunoenzymometric assay kit (Tosoh, Tokyo, Japan) were all undetectable during insulin, clonidine, and GH-releasing hormone provocation tests, whereas urine GH value measured with a Hitachi chemiluminescence enzyme immunoassay kit (Hitachi Chemical) was within the normal range. Serum IGF-1 value was at a low-normal range, and IGF-binding protein-3 (IGFBP-3) was below the normal range. Other pituitary hormones and thyroid hormones were normal. Since these endocrine and auxological data satisfied the criteria for GH therapy in Japan (the criteria in children aged ≥5 years: height, below −2.5 S.D.; peak GH value, below 6.0 ng/ml at least in two provocation tests; and serum IGF-1 value, below 200 ng/ml) (5), recombinant human GH therapy (0.175 mg/kg per week) was started at 7 years and

DOI: 10.1530/EJE-09-0178
Online version via www.eje-online.org

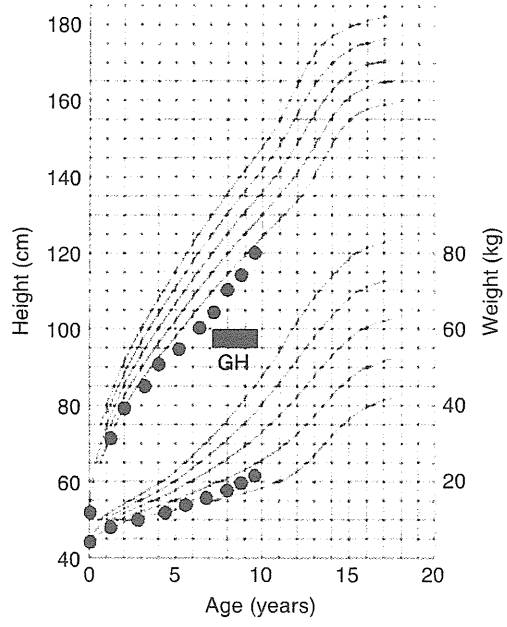

Figure 1 Growth charts of this patient (black circles) plotted on the Japanese sex-matched standard growth curves (+2 S.D., +1 S.D., the mean, −1 S.D., and −2 S.D). The period of GH therapy is indicated.

3 months after consultation with the parents, but the responsiveness to this therapy was not so remarkable (Fig. 1 and Table 2).

Clinical data of the family members are summarized in Table 2. Since endocrine data of the sister and the mother were examined after the investigations of the patient, basal GH values were measured with the Tosoh kit and a Daiichi IRMA kit (Radio Isotope, Tokyo, Japan; endocrine data were not available in the father). In addition, the Daiichi kit was also applied to measure the basal GH in stocked serum samples of the patient, although the serum samples during the provocation tests at 7 years and 1 month of age were not preserved. Notably, the basal GH values of the patient and the sister were obviously different between the two kits, and the GH values in the sister did not show a simple 1:2 ratio between the two kits. The sister and the father had low but normal heights, and the sister had normal endocrine data. The mother had normal clinical findings.

Mutation analysis

This study was approved by the Institutional Review Board Committee at National Center for Child Health and Development. After obtaining written informed consent, leukocyte genomic DNA samples of this patient, the sister, and the parents were amplified by PCR for the coding exons 1–5 and their flanking splice sites of *GH1*, and the PCR products were subjected to direct sequencing on a CEQ 8000 autosequencer (Beckman Coulter, Fullerton, CA, USA). To confirm a heterozygous mutation, the corresponding PCR products were subcloned with a TOPO TA cloning kit (Invitrogen), and wildtype (WT) and mutant (MT) alleles were sequenced separately. The primers used are shown in Table 3, and the primer positions are depicted in Fig. 2A.

Expression analysis

WT-*GH1* from a normal subject and MT-*GH1* from this patient were PCR-amplified with primers GH-1F and GH-5R (Fig. 2A; Table 3) using genomic DNA samples, and the PCR products were subcloned into pCR2.1 plasmid using the TOPO TA cloning kit. Then, *GH1* gene fragments were cleaved from the plasmid DNA with EcoR1 and ligated to the EcoR1 site of an expression vector pRK5. The expression vectors (8 μg) were transiently transfected to SDR-P-1D5 cells obtained from the GH-deficient spontaneous dwarf rat (6),

Table 1 Endocrine studies at 7 years of age.

		Patient		Reference values	
	Stimulus (dosage)	Baseline	Peak	Baseline	Peak
Serum					
GH (ng/ml)[a]	Insulin (0.1 U/kg)	<0.1	<0.1	0.1–20.5	>6.0
	Clonidine (0.1 mg/m^2)	<0.1	<0.1	0.1–20.5	>6.0
	GHRH (1 μg/kg)	<0.1	<0.1	0.1–20.5	>6.0
LH (mIU/ml)	GnRH (100 μg/m^2)	<0.2	5.0	0.0–1.4	0.4–6.0
FSH (mIU/ml)	GnRH (100 μg/m^2)	1.5	19.2	0.6–4.0	6.3–15.6
ACTH (pg/ml)	Insulin (0.1 U/kg)	26.1	179	7.2–22.1	>50
TSH (μU/ml)		1.8		0.44–4.1	
Free T_4 (ng/dl)		1.2		1.03–2.0	
Free T_3 (pg/ml)		3.5		2.40–4.68	
Urine					
GH (pg/mg.cr)[b]		17		>7.0	

Reference values indicate the normal ranges in age-matched Japanese boys (26, 27). Blood sampling during the provocation tests: 0, 15, 30, 60, 90, and 120 mins. IGF-1, insulin-like growth factor-1; T_4, thyroxine; T_3, tri-iodothyronine; and GHRH, growth hormone releasing hormone.
[a]Measured with a Tosoh immunoassay kit.
[b]Measured with a Hitachi immunoassay kit.

Table 2 Summary of clinical data of the family members.

	Patient		Sister	Father	Mother
Age (years)	7 1/12[a]	9 6/12[b]	6 2/12	39	36
Height (cm)	104.5	120.3	105.2	163.0	155.0
Height SDS[c]	−3.0	−2.4	−1.8	−1.5	−0.6
Bone age (years)[d]	3 3/12	5 8/12	NE	NE	NE
GH (ng/ml; Tosoh kit)[e]	<0.1	<0.1[f]	5.23	NE	0.1
GH (ng/ml; Daiichi kit)[e]	1.5	2.86[f]	8.35	NE	0.1
	(0.1–20.5)	(0.1–19.5)	(0.1–21.0)	–	(0.1–3.7)
IGF-1 (ng/ml)	93	140	234	NE	236
	(63–339)	(87–405)	(61–372)	–	(109–265)
IGFBP-3 (ng/ml)	1.36	2.29	2.36	NE	2.79
	(1.76–3.38)	(1.99–3.41)	(1.66–2.91)	–	(1.99–3.19)

IGF-1, insulin-like growth factor-1; IGFBP-3, insulin-like growth factor-binding protein-3; and NE, not examined. The basal hormone values are shown; the values in parentheses represent age- and sex-matched Japanese reference data (26, 27).
[a]Before GH therapy.
[b]On GH therapy.
[c]Assessed by the age- and sex-matched Japanese reference data (28).
[d]Evaluated by the TW-2 method standardized for Japanese (29).
[e]Recombinant GH standard (WHO International Reference Preparation 98/574) has been utilized for the calibration of both kits.
[f]Since blood sample was obtained at 15 h after the GH injection, these values would primarily, if not totally, represent endogenous GH values.

using Gene Pulser Electroporation System (Bio-Rad Laboratories). The transfected cells were incubated for 48 h in a plate with a diameter of 10 cm, and GH in the culture media was measured with the Tosoh and the Daiichi kits. This analysis was performed for three independent experiments. Furthermore, western blotting was performed for the culture media using Rabbit polyclonal GH antibodies (Abs) and anti-Rabbit IgG conjugated with alkaline phosphatase (Promega).

Bioassay

A cell proliferation bioassay was performed for WT-GH and MT-GH, using mouse pro-B cell lymphoma cells that express GH receptor (Ba/F3–hGHR cells) (7). The detailed protocol has been reported previously (8). In brief, WT-GH and MT-GH were prepared in solutions at concentrations of 5, 10, and 20 ng/ml that were determined with the Daiichi kit. Each GH solution of 25 μl was added to 200 μl of Ba/F3–hGHR cell suspension (1×10^5 cells/ml), and the mixture was incubated for 48 h at 37 °C. At the end of the incubation, a colorimetric end point was obtained by an eluted stain bioassay (9), and a bioactive response was determined with a kinetic microplate reader (Molecular Devices, Menlo Park, CA, USA) using optical densities at the test wavelength of 550 nm and a reference wavelength of 650 nm to correct for differential scattering. The experiments were performed in quadruplicate. Statistical significance was examined by Student's *t*-test.

Table 3 Primers utilized in this study.

Primer	Forward Reverse	AT (C) PS (bp)
<Mutation analysis>		
GH-1F	ACAGGTGGGGTCAACAGTGG	60
GH-1R	CCAGGGACCAGGAGCTTTCT	303
GH-2F	CAATCTCAGAAAGCTCCTGG	60
GH-2R	AGCTCCTTAGTCTCCTCCTC	374
GH-3/4F	AGATGAGCACACGCTGAGTG	62
GH-3/4R	AAGGTGAGTTCTCTTGGGTC	584
GH-5F	AGGCCTTTCTCTACACCCTG	60
GH-5R	AGAAGGACACCTAGTCAGAC	435
<Expression analysis>		
GH-1F	ACAGGTGGGGTCAACAGTGG	60
GH-5R	AGAAGGACACCTAGTCAGAC	1727

AT, annealing temperature; and PS, product size.

Protein modeling analysis

The protein conformation was analyzed by Esy-Pred3D (10).

Results

Mutation analysis

Two novel mutations were identified in the patient, a 2 bp deletion at exon 3 (c.280–281delCA) that is predicted to cause a frameshift at the 68th codon for glutamine and resultant termination at the 106th codon (p.Q68fsX106) and a missense mutation at exon 4 (c.426C>G) that is predicted to result in a substitution of aspartic acid with glutamic acid at the 116th codon of GH produced by a novel *GH1* mutation (p.D116E; Fig. 2B). The father and the sister were heterozygous for the p.D116E, and the mother was heterozygous for the p.Q68fsX106 mutation (Fig. 2C).

Functional studies

Expression analysis showed that the p.D116E-GH in the three different culture media was immeasurable with the Tosoh kit but was clearly measurable with the Daiichi kit, and that the p.Q68fsX106-GH was

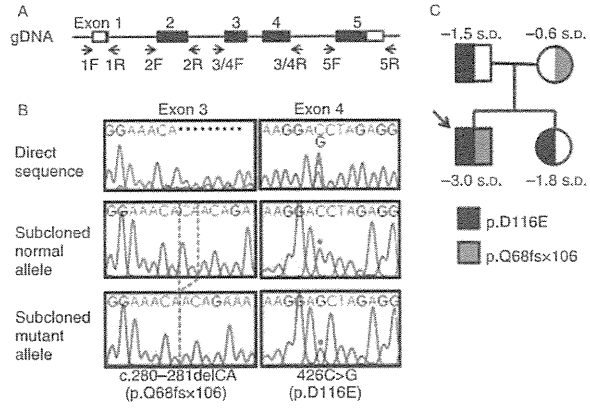

Figure 2 (A) Schematic representation of *GH1*. The black and white boxes on genomic DNA (gDNA) denote the coding regions on exons 1–5 and the UTRs respectively. The arrows indicate the position of the primers utilized in this study. (B) Mutation analysis of *GH1* in this patient. The electrochromatograms delineate the c.280–281delCA (p.Q68fsX106) mutation in exon 3 (left) and the c.426C>G (p.D116E) mutation in exon 4 (right). The mutations have been indicated by the direct sequencing, and confirmed by the subsequently performed sequencing of the subcloned normal and mutant alleles. (C) Pedigree of the family. The height SDS is shown for each family member; for the patient the S.D. before GH therapy is indicated. Of the two mutations identified in this patient, p.D116E is of paternal origin and p.Q68fsX106 is of maternal origin. The sister is heterozygous for the p.D116E mutation.

undetectable by both of the kits (Table 4). Western blot analysis delineated a 22 kDa band for the p.D116E-GH as well as for the WT-GH (Fig. 3A), and a similar band intensity was identified when 3 ng of the p.D116E-GH measured with the Daiichi kit (13 μl of culture media of experiment 3 in Table 4) and 5 ng of WT-GH were utilized. For the p.Q68fsX106-GH, no band was identified for the same amount of culture media (13 μl). Bioassay revealed that the bioactivity was similar between the WT-GH and the p.D116E-GH ($P=0.069$, 0.066, and 0.127 at GH concentrations of 5, 10, and 20 ng/ml based on the Daiichi kit respectively; Fig. 3B). Protein-modeling analysis indicated a normal conformation of the p.D116E-GH (Fig. 3C).

Discussion

This patient had apparently complete GH deficiency and two novel compound *GH1* mutations (p.D116E and p.Q68fsX106). However, his growth pattern including normal birth length, the relatively mild postnatal growth failure, and the poor response to GH therapy is not typical for congenital GH deficiency (11, 12), and the urine GH and serum IGF-1 and IGFBP-3 values indicate a hidden GH activity. Consistent with this, the p.D116E-GH was immeasurable with the Tosoh kit but was measurable with the Daiichi kit, and had an apparently normal *in vitro* biological function. In this regard, the three kits employed in this study utilize two monoclonal

Table 4 GH values in the culture media (ng/ml).

	p.D116E		p.Q68fsX106	
Experiment	Tosoh kit	Daiichi kit	Tosoh kit	Daiichi kit
1	<0.1	90	<0.1	<0.1
2	<0.1	107	<0.1	<0.1
3	<0.1	232	<0.1	<0.1

Abs for GH, one against an epitope within the 22 kDa GH-specific residues (32–46 amino acids) and the other against an epitope specific to each kit. The Hitachi kit detects an epitope at the N-terminal region, while the epitope specifically recognized by the Tosoh and Daiichi kits is unknown. Thus, while the p.Q68fsX106 appears to be an amorphic mutation that is incapable of producing GH probably because of nonsense-mediated mRNA decay (13), it is likely that the p.D116E affects the GH epitope primarily recognized by the Tosoh kit but not by the Hitachi or the Daiichi kit, thereby producing a possible immunologically anomalous but biologically active GH. This notion would also explain why the basal serum GH values measured with the Tosoh kit were obviously lower than those measured with the Daiichi kit in the patient and the sister with p.D116E.

It remains to be determined, however, whether the p.D116E-GH has a normal biological function *in vivo*. Although the *in vitro* bioassay indicated an apparently normal function for the p.D116E-GH, it is known that

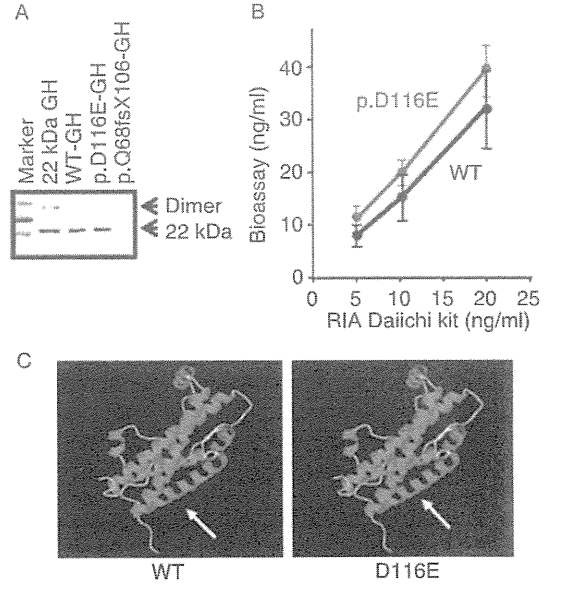

Figure 3 (A) Western blot analysis, showing the presence of 22 kDa WT-GH and p.D116E-GH. The standard 22 kDa human GH is used as an internal control (8). Note that a similar band intensity is delineated for 3 ng of the p.D116E-GH and 5 ng of WT-GH measured with the Daiichi kit. (B) Bioassay of the WT-GH and the p.D116E-GH, using Ba/F3–hGH receptor cells. The results are expressed using the mean and the S.D. (C) Ribbon diagrams of the GH proteins. The white arrows indicate the 116 residue for WT-GH and the p.D116E-GH.

the results obtained with artificially constructed cell lines do not necessarily reflect the *in vivo* biological effects of hGH MTs (8, 14). Indeed, the difference in the GH value between the two kits in the sister and the relationship between the GH value and the band intensity in the western blotting may imply that the p.D116E-GH was not measured precisely even with the Daiichi kit, so that a relatively large amount of the p.D116E-GH was probably utilized in the *in vitro* bioassay, compensating for a possible hypofunction of the p.D116E-GH. Furthermore, since the previously described p.D116A-GH harboring a missense mutation within the GH receptor-binding site 2 has a 5.7-fold lower affinity to the GH receptor than the WT-GH (15), this would argue for a functional importance of the D116 residue and implicate a similar functional alteration of the p.D116E-GH. In addition, although *GH1* missense mutations reported to date are relatively rare (16), GH missense MTs, including those within or near the GH receptor binding site 2, frequently have a reduced or altered biological activity (2, 4, 17–21).

In this regard, comparison of clinical data between the patient with functional hemizygosity for the p.D116E and the mother with functional hemizygosity for the WT *GH1* would suggest that the p.D116E-GH has a reduced, though not abolished, *in vivo* bioactivity (Table 2). In support of this, most individuals with heterozygous *GH1* deletions have normal stature (22) as observed in the mother, while this patient had short stature. It may also be possible that the p.D116E-GH is less secreted from the pituitary into the circulation when compared with an intact GH protein, although the clinical findings of the father and the sister heterozygous for the p.D116E would argue against the possibility that the p.D116E-GH exerts an obvious dominant negative effect (Table 2). However, since short stature is a highly heterogeneous phenotype subject to multiple genetic and environmental factors (23, 24), some factors other than the *GH1* mutations may be involved in the development of short stature in this patient. In addition, there may be an ascertainment bias, because GH-related studies are almost exclusively performed in individuals with short stature. Further studies will permit to clarify the *in vivo* biological function of the p.D116E-GH and its relevance to the development of short stature.

Such an immunologically anomalous and biologically active hormone has been reported previously. It is known that the common LH variant (V-LH) with two completely linked Trp8Arg and Ile15Thr substitutions in the LHβ-subunit is immunologically undetectable when a MAB recognizing an epitope present in the intact LH α/β dimer is utilized, but is measurable when two monoclonal Abs recognizing specific sites in the LHβ subunit are utilized (25). Notably, the V-LH appears to have somewhat weaker bioactivity than the WT-LH, and is often associated with the primary ovarian dysfunction in the Japanese population (25). Nevertheless, elevated LH values characteristic of primary ovarian dysfunction cannot be identified without applying the method using two monoclonal Abs, although FSH values are definitely increased. Thus, when a discrepancy is present between values of a specific hormone and other biochemical data or clinical findings, it is recommended to measure the specific hormone with a different kit, to avoid the misdiagnosis of hormone deficiency.

In summary, we identified an immunologically anomalous but considerably bioactive GH produced by p.D116E mutation. Indeed, such abnormalities along the GH/IGF-1 axis may also be identified by performing GH-related endocrine studies in children with short stature. The presence of such an apparently immeasurable but bioactive hormone, as well as a measurable but bioinactive hormone, should be kept in mind, to allow for an appropriate assessment of endocrine data.

Declaration of interest

The authors declare no conflict of interest.

Funding

This research was supported by Grants for Child Health and Development and Research on Children and Families from the Ministry of Health, Labor, and Welfare.

References

1 Growth Hormone Research Society. Consensus guidelines for the diagnosis and treatment of growth hormone (GH) deficiency in childhood and adolescence: summary statement of the GH Research Society. *Journal of Clinical Endocrinology and Metabolism* 2000 **85** 3990–3993.

2 Takahashi Y, Shirono H, Arisaka O, Takahashi K, Yagi T, Koga J, Kaji H, Okimura Y, Abe H, Tanaka T & Chihara K. Biologically inactive growth hormone caused by an amino acid substitution. *Journal of Clinical Investigations* 1997 **100** 1159–1165.

3 Besson A, Salemi S, Deladoëy J, Vuissoz JM, Eblé A, Bidlingmaier M, Bürgi S, Honegger U, Flück C & Mullis PE. Short stature caused by a biologically inactive mutant growth hormone (GH-C53S). *Journal of Clinical Endocrinology and Metabolism* 2005 **90** 2493–2499.

4 Millar DS, Lewis MD, Horan M, Newsway V, Easter TE, Gregory JW, Fryklund L, Norin M, Crowne EC, Davies SJ, Edwards P, Kirk J, Waldron K, Smith PJ, Phillips JA III, Scanlon MF, Krawczak M, Cooper DN & Procter AM. Novel mutations of the growth hormone 1 (GH1) gene disclosed by modulation of the clinical selection criteria for individuals with short stature. *Human Mutation* 2003 **21** 424–440.

5 Tanae A, Macsaka I, Tanaka T, Yokoya S & Tachibana K. *Therapy for Pediatric Endocrinological Disease*, pp. 1–3, Tokyo: Shindan to Chiryou, 2007 (in Japanese).

6 Nogami H, Takeuchi T, Suzuki K, Okuma S & Ishikawa H. Studies on prolactin and growth hormone gene expression in the pituitary gland of spontaneous dwarf rats. *Endocrinology* 1989 **125** 964–970.

7 Wada M, Uchida H, Ikeda M, Tsunekawa B, Naito N, Banba S, Tanaka E, Hashimoto Y & Honjo M. The 20 kDa human growth hormone (hGH) differs from the 22 kDa hGH in the complex

formation with cell surface hGH receptor and hGH-binding protein circulating in human plasma. *Molecular Endocrinolgy* 1998 **12** 146–156.
8 Ishikawa M, Nimura A, Horikawa R, Katsumata N, Arisaka O, Wada M, Honjo M & Tanaka T. A novel specific bioassay for serum human growth hormone. *Journal of Clinical Endocrinology and Metabolism* 2000 **85** 4274–4279.
9 Ealey PA, Yateman ME, Sandhu R, Dattani MT, Hassan MK, Holt SJ & Marshall NJ. The development of an eluted stain bioassay (ESTA) for human growth hormone. *Growth Regulation* 1995 **5** 36–44.
10 Lambert C, Léonard N, De Bolle X & Depiereux E. ESyPred3D: prediction of proteins 3D structures. *Bioinformatics* 2002 **18** 1250–1256.
11 Laron Z & Silbergeld A. A simple diagnostic screening test for children with short stature – with emphasis on genetic defects along the GH axis. *Pediatric Endocrinology Reviews* 2007 **4** 96–98.
12 Tanaka T, Cohen P, Clayton PE, Laron Z, Hintz RL & Sizonenko PC. Diagnosis and management of growth hormone deficiency in childhood and adolescence – part 2: growth hormone treatment in growth hormone deficient children. *Growth Hormone and IGF Research* 2002 **12** 323–341.
13 Holbrook JA, Neu-Yilik G, Hentze MW & Kulozik AE. Nonsense-mediated decay approaches the clinic. *Nature Genetics* 2004 **36** 801–808.
14 Popii V & Baumann G. Laboratory measurement of growth hormone. *Clinica Chimica Acta* 2004 **350** 1–16.
15 Cunningham BC, Ultsch M, De Vos AM, Mulkerrin MG, Clauser KR & Wells JA. Dimerization of the extracellular domain of the human growth hormone receptor by a single hormone molecule. *Science* 1991 **254** 821–825.
16 Wagner JK, Eblé A, Hindmarsh PC & Mullis PE. Prevalence of human GH-1 gene alterations in patients with isolated growth hormone deficiency. *Pediatric Research* 1998 **43** 105–110.
17 Lewis MD, Horan M, Millar DS, Newsway V, Easter TE, Fryklund L, Gregory JW, Norin M, Del Valle CJ, López-Siguero JP, Cañete R, López-Canti LF, Díaz-Torrado N, Espino R, Ulied A, Scanlon MF, Procter AM & Cooper DN. A novel dysfunctional growth hormone variant (Ile179Met) exhibits a decreased ability to activate the extracellular signal-regulated kinase pathway. *Journal of Clinical Endocrinology and Metabolism* 2004 **89** 1068–1075.
18 Binder G, Keller E, Mix M, Massa GG, Stokvis-Brantsma WH, Wit JM & Ranke MB. Isolated GH deficiency with dominant inheritance: new mutations, new insights. *Journal of Clinical Endocrinology and Metabolism* 2001 **86** 3877–3881.
19 Deladoëy J, Stocker P & Mullis PE. Autosomal dominant GH deficiency due to an Arg183His GH-1 gene mutation: clinical and molecular evidence of impaired regulated GH secretion. *Journal of Clinical Endocrinology and Metabolism* 2001 **86** 3941–3947.
20 Salemi S, Yousefi S, Baltensperger K, Robinson IC, Eblé A, Simon D, Czernichow P, Binder G, Sonnet E & Mullis PE. Variability of isolated autosomal dominant GH deficiency (IGHD II): impact of the P89L GH mutation on clinical follow-up and GH secretion. *European Journal of Endocrinology* 2005 **153** 791–802.
21 Dattani MT, Hindmarsh PC, Brook CG, Robinson IC, Kopchick JJ & Marshall NJ. G120R, a human growth hormone antagonist, shows zinc-dependent agonist and antagonist activity on Nb2 cells. *Journal of Biological Chemistry* 1995 **270** 9222–9226.
22 Phillips JA III & Cogan JD. Genetic basis of endocrine disease. 6. Molecular basis of familial human growth hormone deficiency. *Journal of Clinical Endocrinology and Metabolism* 1994 **78** 11–16.
23 Visscher PM. Sizing up human height variation. *Nature Genetics* 2008 **40** 489–490.
24 Vogel F & Motulsky AG. *Human Genetics: Problems and Approaches* Berlin/Heidelberg/New York/Tokyo: Springer-Verlag, 1986.
25 Themmen APN & Huhtaniemi IT. Mutations of gonadotropins and gonadotropin receptors: elucidating the physiology and pathophysiology of pituitary–gonadal function. *Endocrine Reviews* 2000 **21** 551–583.
26 Japan Public Health Association. *Normal Biochemical Values in Japanese Children* Tokyo: Sanko Press, 1996 (in Japanese).
27 Inada H, Imamura T & Nakajima R. *Manual of Endocrine Examination for Children*, pp. 14–22, Osaka: Medical Review, 2002 (in Japanese).
28 Suwa S, Tachibana K, Maesaka H, Tanaka T & Yokoya S. Longitudinal standards for height and height velocity for Japanese children from birth to maturity. *Clinical Pediatric Endocrinology* 1992 **1** 5–13.
29 Murata M, Matsuo N, Tanaka T, Ohtsuki F, Ashizawa K, Tatara H, Anzo M, Sato M, Matsuoka H, Asami T & Tsukakoshi K. *Radiographic Atlas of Skeletal Development for the Japanese* Tokyo: Kanehara Press, 1993 (in Japanese).

Received 19 May 2009
Accepted 19 May 2009

Heterozygous Orthodenticle Homeobox 2 Mutations Are Associated with Variable Pituitary Phenotype

Sumito Dateki, Kitaro Kosaka, Kosei Hasegawa, Hiroyuki Tanaka, Noriyuki Azuma, Susumu Yokoya, Koji Muroya, Masanori Adachi, Toshihiro Tajima, Katsuaki Motomura, Eiichi Kinoshita, Hiroyuki Moriuchi, Naoko Sato, Maki Fukami, and Tsutomu Ogata

Department of Endocrinology and Metabolism (S.D., N.S., M.F., T.O.), National Research Institute for Child Health and Development, and Division of Ophthalmology (N.A.) and Department of Medical Subspecialties (S.Y.), National Children's Medical Center, Tokyo 157-8535, Japan; Department of Pediatrics (S.D., K.M., E.K., H.M.), Nagasaki University Graduate School of Biomedical Sciences, Nagasaki 852-8501, Japan; Department of Pediatrics (K.K.), Kyoto Prefectural University of Medicine, Graduate School of Medical Science, Kyoto 602-8566, Japan; Department of Pediatrics (K.H., H.T.), Okayama University Graduate School of Medicine, Dentistry, and Pharmaceutical Sciences, Okayama 700-8558, Japan; Division of Endocrinology and Metabolism (K.M., M.A.), Kanagawa Children's Medical Center, Yokohama 232-8555, Japan; and Department of Pediatrics (T.T.), Hokkaido University School of Medicine, Sapporo 060-8638, Japan

Context: Although recent studies have suggested a positive role of *OTX2* in pituitary as well as ocular development and function, detailed pituitary phenotypes in *OTX2* mutations and *OTX2* target genes for pituitary function other than *HESX1* and *POU1F1* remain to be determined.

Objective: We aimed to examine such unresolved issues.

Subjects: We studied 94 Japanese patients with various ocular or pituitary abnormalities.

Results: We identified heterozygous p.K74fsX103 in case 1, p.A72fsX86 in case 2, p.G188X in two unrelated cases (3 and 4), and a 2,860,561-bp microdeletion involving *OTX2* in case 5. Clinical studies revealed isolated GH deficiency in cases 1 and 5; combined pituitary hormone deficiency in case 3; abnormal pituitary structures in cases 1, 3, and 5; and apparently normal pituitary function in cases 2 and 4, together with ocular anomalies in cases 1–5. The wild-type Orthodenticle homeobox 2 (OTX2) protein transactivated the *GNRH1* promoter as well as the *HESX1*, *POU1F1*, and *IRBP* (interstitial retinoid-binding protein) promoters, whereas the p.K74fsX103-OTX2 and p.A72fsX86-OTX2 proteins had no transactivation functions and the p.G188X-OTX2 protein had reduced (~50%) transactivation functions for the four promoters, with no dominant-negative effect. cDNA screening identified positive *OTX2* expression in the hypothalamus.

Conclusions: The results imply that *OTX2* mutations are associated with variable pituitary phenotype, with no genotype-phenotype correlations, and that *OTX2* can transactivate *GNRH1* as well as *HESX1* and *POU1F1*. **(*J Clin Endocrinol Metab* 95: 756–764, 2010)**

Pituitary development and function depends on the spatially and temporally controlled expression of multiple transcription factor genes such as *POU1F1*, *HESX1*, *LHX3*, *LHX4*, *PROP1*, and *SOX3* (1, 2). Whereas mutations of some genes (*e.g. POU1F1*) result in a relatively characteristic pattern of pituitary hormone deficiency, those of other genes (*e.g. HESX1*) are associated with a wide range of pituitary phenotype including combined pi-

ISSN Print 0021-972X ISSN Online 1945-7197
Printed in U.S.A.

doi: 10.1210/jc.2009-1334 Received June 23, 2009. Accepted November 9, 2009.
First Published Online December 4, 2009

Abbreviations: CGH, Comparative genomic hybridization; CPHD, combined pituitary hormone deficiency; EPP, ectopic posterior pituitary; FISH, fluorescence *in situ* hybridization; HD, homeodomain; IGHD, isolated GH deficiency; IRBP, interstitial retinoid-binding protein; MLPA, multiplex ligation-dependent probe amplification; NMD, nonsense mediated mRNA decay; OTX2, orthodenticle homeobox 2; PH, pituitary hypoplasia; SOD, septooptic dysplasia; TD, transactivation domain.

tuitary hormone deficiency (CPHD), isolated GH deficiency (IGHD), and apparently normal phenotype. However, because mutations of these genes account for a relatively minor portion of patients with congenital hypopituitarism (2, 3), multiple genes would remain to be identified in congenital hypopituitarism.

Orthodenticle homeobox 2 (*OTX2*) is a transcription factor gene primarily involved in ocular development (4). It encodes a paired type homeodomain (HD) and a transactivation domain (TD) and produces two functionally similar splice variants, isoform-a (GenBank accession no. NM_21728.2) and isoform-b (NM_172337.1) with and without eight amino acids because of alternative splice acceptor sites at the boundary of intron 3 and exon 4 (5). To date, at least 10 pathological heterozygous *OTX2* mutations have been identified in patients with ocular malformations such as anophthalmia and/or microphthalmia (6, 7). Ocular phenotype is highly variable, ranging from anophthalmia to nearly normal eye development, even in patients from the same family. Furthermore, most patients also exhibit brain anomaly, seizure, and/or developmental delay.

Recent studies have indicated that *OTX2* is also involved in pituitary development and function. Dateki *et al.* (8) showed that *OTX2* is expressed in the pituitary and has a transactivation function for the promoters of *POU1F1* and *HESX1* as well as the promoter of *IRBP* (interstitial retinoid-binding protein) involved in ocular function and that a frameshift *OTX2* mutation identified in a patient with bilateral anophthalmia and partial IGHD barely retained the transactivation activities. Subsequently a missense *OTX2* mutation with a dominant-negative effect and a frameshift *OTX2* mutation with loss-of-function effect were identified in CPHD patients with and without ocular malformation (9, 10).

However, detailed pituitary phenotypes in *OTX2* mutation-positive patients as well as other possible *OTX2* target genes for pituitary development and function remain to be determined. Here we report five new patients with *OTX2* mutations and summarize clinical findings in *OTX2* mutation-positive patients. We also show that *OTX2* is expressed in the hypothalamus and has a transactivation function for the promoter of *GNRH1*.

Patients and Methods

Patients

We studied 94 Japanese patients consisting of: 1) 16 patients with ocular anomalies and pituitary dysfunctions accompanied by short stature (<−2 SD) (six with anophthalmia and/or microphthalmia and CPHD, five with anophthalmia and/or microphthalmia and IGHD, three with septooptic dysplasia (SOD) and CPHD, and two with SOD and IGHD) (group 1); 2) 12 patients with ocular anomalies whose pituitary functions were not investigated (one with bilateral microphthalmia and short stature, one with bilateral optic nerve hypoplasia and short stature, and 10 with anophthalmia and/or microphthalmia and normal stature) (group 2); and 3) 66 patients with pituitary dysfunctions but without ocular anomalies (five with IGHD and 61 patients with CPHD) (group 3). No demonstrable mutation was identified for *HESX1* in patients with SOD, *GH1* and *HESX1* in patients with IGHD, and *POU1F*, *HESX1*, *LHX3*, *LHX4*, *PROP1*, and *SOX3* in patients with various types of CPHD (2). All the patients had normal karyotype.

Primers and probes

The primers and probes used in this study are shown in Supplemental Table 1, published as supplemental data on The Endocrine Society's Journals Online web site at http://jcem.endojournals.org.

Sequence analysis of OTX2

This study was approved by the Institutional Review Board Committee at National Center for Child Health and Development. After obtaining written informed consent, the coding exons 3-5 and their flanking splice sites were PCR amplified using leukocyte genomic DNA samples of all 94 patients and were subjected to direct sequencing on a CEQ 8000 autosequencer (Beckman Coulter, Fullerton, CA). To confirm a heterozygous mutation, the corresponding PCR products were subcloned with TOPO TA cloning kit (Invitrogen, Carlsbad, CA), and normal and mutant alleles were sequenced separately.

Prediction of the occurrence of aberrant splicing and nonsense mediated mRNA decay (NMD)

To examine whether identified mutations could cause aberrant splicing by creating or disrupting exonic splicing enhancers and/or splice sites (11, 12), we performed *in silico* analyses with the ESE finder release 3.0 (http://rulai.cshl.edu/cgi-bin/tools/ESE3/esefinder.cgi) for the prediction of exonic splice enhancers and with the program at the Berkeley Drosophila Genome Project (http://www.fruitfly.org/seq_tools/splice.html) for the prediction of splice sites. We also analyzed whether identified mutations could be subject to NMD on the basis of the previous report (12, 13).

Deletion analysis

Multiplex ligation-dependent probe amplification (MLPA) was performed for *OTX2* intragenic mutation-negative patients as a screening of a possible microdeletion affecting *OTX2*. This procedure was performed according to the manufacturer's instructions (14), using probes designed specifically for *OTX2* exon 4 together with a commercially available MLPA probe mix (P236) (MRC-Holland, Amsterdam, The Netherlands) used as internal controls. To confirm a microdeletion, fluorescence *in situ* hybridization (FISH) was performed with a long PCR product for *OTX2* (a 6096 bp segment from intron 2 to exon 5) together with an RP11-566I2 BAC probe (14q11.2; Invitrogen, Carlsbad, CA) used as an internal control. The probe for *OTX2* was labeled with digoxigenin and detected by rhodamine anti-digoxigenin, and the control probe was labeled with biotin and

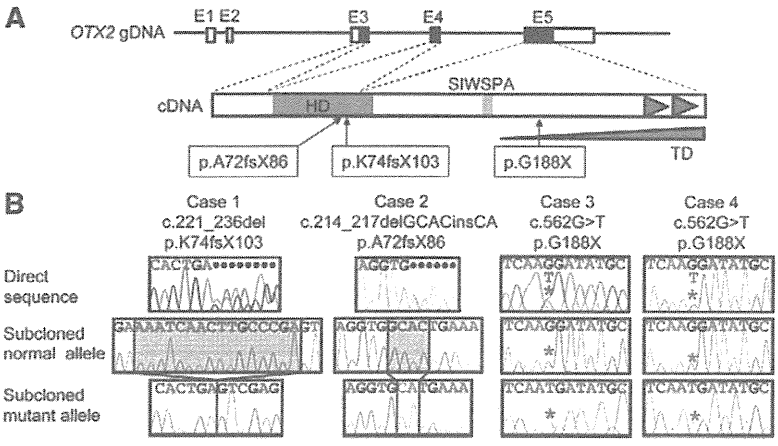

FIG. 1. Sequence analysis in cases 1–4. A, The structure of *OTX2* (the isoform-b) and the position of the mutations identified. The *black* and *white boxes* on genomic DNA (gDNA) denote the coding regions on exons 1-5 (E1-E5) and the untranslated regions, respectively. *OTX2* encodes the HD (a *blue region*), the SIWSPA conserved motif (an *orange region*), and the two tandem tail motifs (*green triangles*). The TD (a *gray triangle*) is assigned to the C-terminal side; deletion of each tail motif reduces the transactivation function, and that of a region distal to the SIWSPA motif further reduces the transactivation function. In addition, another TD may also reside in the 5′ side of the HD (17). The three mutations identified in this study are shown. B, Electrochromatograms showing the mutations in cases 1–4. Shown are the direct sequences and subcloned normal and mutant sequences. The deleted sequences are shaded in *gray*, and the inserted sequence is highlighted in *yellow*. The mutant and the corresponding wild-type nucleotides are indicated by *red asterisks*.

detected by avidin conjugated to fluorescein isothiocyanate. To indicate an extent of a microdeletion, oligoarray comparative genomic hybridization (CGH) was carried out with 1×244K human genome array (catalog no. G4411B; Agilent Technologies, Palo Alto, CA), according to the manufacturer's protocol. Finally, to characterize a microdeletion, long PCR was performed with primer pairs flanking the deleted region, and a long PCR product was subjected to direct sequencing using serial sequence primers. The deletion size and the junction structure were determined by comparing the obtained sequences with the reference sequences at the National Center for Biotechnology Information Database (NC_000014.7; Bethesda, MD), and the presence or absence of repeat sequences around the breakpoints was examined with Repeatmasker (http://www.repeatmasker.org).

Functional studies

Western blot analysis, subcellular localization analysis, DNA binding analysis, and transactivation analysis were performed by the previously reported methods (8) (for details, see Supplemental Methods). In this study, we used the previously reported expression vector and fluorescent vector containing the wild-type *OTX2* cDNA; the probes with the wild-type and mutated OTX2 binding sites within the *IRBP*, *HESX1*, and *POU1F1* promoter sequences; and the luciferase reporter vectors containing the *IRBP*, *HESX1*, and *POU1F1* promoter sequences (8). We further created expression vectors and fluorescent vectors containing mutant *OTX2* cDNAs by site-directed mutagenesis using Prime STAR mutagenesis basal kit (Takara, Otsu, Japan), and constructed a 30-bp probe with wild-type (TAATCT) and mutated (TGGGCT) putative OTX2 binding site within the *GNRH1* promoter sequence and a luciferase reporter vector containing the *GNRH1* promoter sequence (−1349 to −1132 bp) by inserting the corresponding sequence into pGL3 basic. The *GNRH1* promoter sequence was based on the report of Kelley *et al.* (15). Transfections were performed in triplicate within a single experiment, and the experiment was repeated three times.

PCR-based expression analysis of *OTX2*

Human cDNA samples were purchased from CLONTECH (Palo, Alto, CA) except for leukocyte and skin fibroblast cDNA samples that were prepared with Superscript III reverse transcriptase (Invitrogen). PCR amplification was performed for the cDNA samples (0.5 ng), using the primers hybridizing to exon 3 and 4 of *OTX2* and those hybridizing to exons 2/3 and 4/5 (boundaries) of *GAPDH* used as an internal control.

Results

Identification of mutations and substitutions

Three novel heterozygous *OTX2* mutations were identified in four cases, *i.e.* a 16-bp deletion at exon 4 that is predicted to cause a frameshift at the 74th codon for lysine and resultant termination at the 103rd codon (c.221_236del16, p.K74fsX103) in case 1; a 4-bp deletion and a 2-bp insertion at exon 4 that is predicted to cause a frame shift at the 72nd codon for alanine and resultant termination at the 86th codon (c.214_217delGCACinsCA, p.A72fsX86) in case 2; and a nonsense mutation at exon 5 that is predicted to cause a substitution of the 188th glycine with stop codon (c.562G>T, p.G188X) in two unrelated cases (3 and 4; Fig. 1). In addition, heterozygous missense substitutions were identified in patient 1 (c.532A>T, p.T178S) and patient 2 (c.734C>T, p.A245V). Cases 1 and 3 were from group 1, cases 2 and 4 and patient 2 were from group 2, and patient 1 was from group 3. Parental analysis indicated that frameshift mutations in cases 1 and 2 were absent from the parents (*de novo* mutations), whereas the missense substitution of patient 2 was inherited from phenotypically normal father. The parents of cases 3 and 4 and patient 1 refused molecular studies. All the mutations and the missense substitutions were absent from 100 control subjects.

Prediction of the occurrence of aberrant splicing and NMD

The two frameshift mutations and the nonsense mutation were predicted to influence neither exonic splice enhancers nor splice donor and acceptor sites (Supplemental Tables 2 and 3). Furthermore, the two frameshift mutations were predicted to produce the premature termination codons on the mRNA transcribed from the last exon

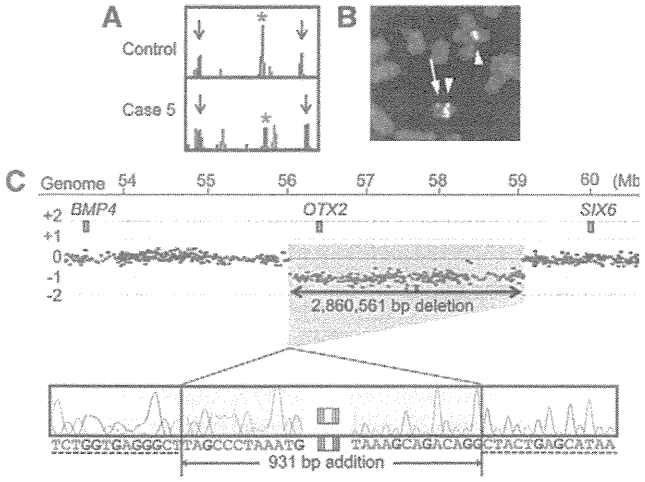

FIG. 2. Deletion analysis in case 5. A, MLPA analysis. The *red asterisk* indicates peaks for the *OTX2* exon 4, and the *black arrows* indicate control peaks. The *red peaks* indicate the internal size markers. Deletion of the MLPA probe binding site is indicated by the reduced peak height. B, FISH analysis. The probe for *OTX2* detects only a *single red signal* (an *arrow*), whereas the RP11-566I2 BAC probe identifies *two green signals* (*arrowheads*). C, Oligoarray CGH analysis and direct sequencing of the deletion junction. The deletion is 2,860,561 bp in physical size (shaded in *gray*) and is associated with an addition of a 931-bp segment (highlighted in *yellow*). The normal sequences flanking the microdeletion are indicated with *dashed underlines*.

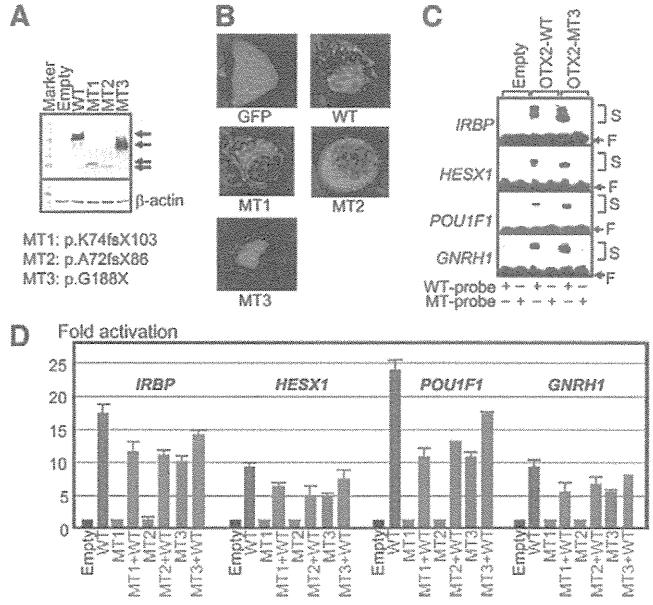

FIG. 3. Functional studies. A, Western blot analysis. Both WT and MT1-MT3 OTX2 proteins are detected with different molecular masses (*arrows*). WT, Wild type; MT1, p.K74fsX103; MT2, p.A72fsX86; and MT3, p.G188X. B, Subcellular localization analysis. Whereas green fluorescent protein (GFP) alone is diffusely distributed throughout the cell, the GFP-fused WT-OTX2 and MT3-OTX2 proteins localize to the nucleus. By contrast, the GFP-fused MT1-OTX2 and MT2-OTX2 proteins are incapable of localizing to the nucleus. C, DNA binding analysis using the wild-type (WT) and mutated (MT) probes derived from the promoters of *IRBP*, *HESX1*, *POU1F1*, and *GNRH1*. The symbols (+) and (–) indicate the presence and absence of the corresponding probes, respectively. Both WT and MT3 OTX2 proteins bind to the WT but not the MT probes. For the probe derived from the *IRBP* promoter, two shifted bands are found for both WT-OTX2 and MT3-OTX2 proteins as reported previously (17). S, Shifted bands; F, free probes. D, Transactivation analysis, using the promoter sequences of *IPBP*, *HESX1*, *POU1F1*, and *GNRH1*. The results are expressed using the mean and SD. The *black*, *blue*, *red*, and *green bars* indicate the data of the empty expression vectors (0.6 μg), expression vectors with WT *OTX2* cDNA (0.6 μg), expression vectors with MT1-MT3 *OTX2* cDNAs (0.6 μg), and the mixture of expression vectors with WT (0.3 μg) and those with MT1-MT3 *OTX2* cDNAs (0.3 μg), respectively; thus, the same amount of expression vectors has been used for each assay.

5, indicating that the frameshift mutations as well as the nonsense mutation had the property to escape NMD (Supplemental Fig. 1).

Identification of a microdeletion

A heterozygous microdeletion affecting *OTX2* was indicated by MLPA and confirmed by FISH in case 5 of group 1 (Fig. 2, A and B). Oligoarray CGH delineated an approximately 2.9-Mb deletion, and sequencing of the fusion point showed that the microdeletion was 2,860,561 bp in physical size (56,006,531–58,867,091 bp on the NC_000014.7) and was associated with an addition of a complex 931-bp segment consisting of the following structures (cen → tel): 2 bp (TA) insertion → 895 bp sequence identical with that in a region just centromeric to the microdeletion (55, 911, 347–55, 912, 241 bp) → 1 bp (C) insertion → 33-bp sequence identical with that within the deleted region (58, 749, 744–58, 749, 776 bp) (Fig. 2C). Repeat sequences were absent around the break points. This microdeletion was not detected in DNA from the parents.

Functional studies of the wild-type and mutant OTX2 proteins

Western blot analysis detected wild-type OTX2 protein of 31.6 kDa and mutant OTX2 proteins of 11.5 kDa (p.K74fsX103), 9.7 kDa (p.A72fsX86), and 15.4 kDa (p.G188X) (Fig. 3A). The molecular masses were as predicted from the mutations. The band intensity was comparable between the wild-type OTX2 protein and the p.G188X-OTX2 protein and was faint for the p.K74fsX103-OTX2 and p.A72fsX86-OTX2 proteins.

Subcellular localization analysis showed that the p.G188X-OTX2 protein localized to the nucleus as did the wild-type OTX2 protein, whereas the p.K74fsX103-OTX2 and p.A72fsX86-OTX2 proteins were incapable of localizing to the nucleus (Fig. 3B). The results were consistent with those of the Western blot analysis because nuclear extracts were used for the Western blotting, with some probable contamination of cytoplasm.

DNA binding analysis revealed that the p.G188X-OTX2 protein with nuclear localizing capacity bound to the wild-type OTX2 binding sites within the four promoters examined, including the *GNRH1* promoter, but not to the mutated OTX2 binding sites (Fig. 3C). The band shift

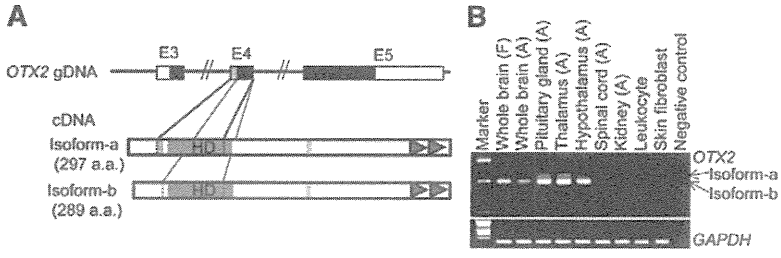

FIG. 4. PCR-based human cDNA library screening for *OTX2* (35 cycles). A, Schematic representation of the *OTX2* isoform-a (NM_21728.2) and isoform-b (NM_172337.1). Because of the two alternative splice acceptor sites at the boundary between intron 3 and exon 4, isoform-a carries eight amino acids (shown in *gray*) in the vicinity of the HD, whereas isoform-b is lacking the eight amino acids. B, PCR amplification data. *OTX2* is clearly expressed in the pituitary and hypothalamus, with isoform-b being the major product. *GAPDH* has been used as an internal control. F, Fetus; A, adult.

was more obvious for the wild-type OTX2 protein than for the p.G188X-OTX2 protein, consistent with the difference in the molecular masses.

Transactivation analysis showed that the wild-type OTX2 protein had transactivation activities for the four promoters examined including the *GNRH1* promoter, whereas the p.K74fsX103-OTX2 and p.A72fsX86-OTX2 proteins had virtually no transactivation function, and the p.G188X-OTX2 protein had reduced (~50%) transactivation activities (Fig. 3D). The three mutant OTX2 proteins had no dominant-negative effects. In addition, the two missense p.A245V-OTX2 and p.T178S-OTX2 proteins had apparently normal transactivation activities with no dominant-negative effect (Supplemental Fig. 2).

PCR-based expression analysis of *OTX2*

OTX2 expression was identified in the pituitary and the hypothalamus as well as in the brain and the thalamus but not detected in the spinal cord, kidney, leukocytes, and skin fibroblasts (Fig. 4). The isoform-b lacking the eight amino acids was predominantly expressed.

Clinical findings in *OTX2* mutation-positive patients

Clinical data are summarized in Table 1 (*left part*). Anophthalmia and/or microphthalmia was present in cases 1–5. Developmental delay was obvious in cases 1 and 3–5, whereas it was obscure in case 2 because of the young age. Prenatal growth was normally preserved in cases 1–5, whereas postnatal growth was compromised in cases 1, 3, and 5. Cases 1 and 5 had IGHD, and case 3 had CPHD (Table 2); furthermore, cases 1, 3, and 5 had pituitary hypoplasia (PH) and/or ectopic posterior pituitary (EPP) (Supplemental Fig. 3). Case 3 showed no pubertal development at 15 yr of age (Tanner pubic hair stage 2 in Japanese boys: 12.5 ± 0.9 yr) (16). Cases 2 and 4 had no discernible pituitary dysfunction and did not receive magnetic resonance imaging examinations. In addition, case 1 had right retractile testis. Patient 1 with p.T178S had CPHD but without ocular anomalies, and patient 2 with p.A245V had bilateral optic nerve hypoplasia and short stature.

Discussion

We identified two frameshift mutations in cases 1 and 2 and a nonsense mutation in unrelated cases 3 and 4. Furthermore, it was predicted that these mutations neither affected splice patterns nor underwent NMD, although direct analysis using mRNA was impossible due to lack of detectable *OTX2* expression in already collected leukocytes as well as skin fibroblasts, which might be available from cases 1–4. Thus, these mutations are predicted to produce aberrant OTX2 proteins *in vivo* that were used in the *in vitro* functional studies. In this context, the functional studies indicated that the two frameshift mutations were amorphic and the nonsense mutation was hypomorphic. The results are consistent with the previous notion that the HD not only has DNA binding capacity but also retains at least a part of nuclear localization signal on its C-terminal portion and the TD primarily resides in the C-terminal region (17) (Fig. 1A). Whereas the two missense substitutions were absent in 100 control subjects, they would be rare normal variations rather than pathological mutations because of the normal transactivation activities with no dominant-negative effect.

We also detected a heterozygous microdeletion involving *OTX2* in case 5 that was not mediated by repeat sequences. This implies the importance of the examination of a microdeletion. Indeed, such a cryptic microdeletion has been identified in multiple genes with the development of MLPA that can serve as a screening method in the detection of microdeletions (18). Whereas the microdeletion of case 5 has removed 16 additional genes (Ensembl Genome Browser, http://www.ensembl.org/), the clinical phenotype of case 5 is explainable by *OTX2* haploinsufficiency alone. Thus, hemizygosity for the 16 genes would not have a major clinical effect, if any.

Furthermore, the present study revealed two findings. First, *OTX2* was expressed in the hypothalamus and had a transactivation function for the *GNRH1* promoter. This implies that *GNRH1* essential for the hypothalamic GnRH secretion is also a target gene of *OTX2*, as has been demonstrated in the mouse (15). Second, the short isoform-b was predominantly identified in the *OTX2* expression-positive tissues. This sug-

TABLE 1. Summary of clinical findings in patients with heterozygous *OTX2* mutations

	Present study					Previous studies[a]			
	Case 1	**Case 2**	**Case 3**	**Case 4**	**Case 5**	**Case 6**	**Case 7**	**Case 8**	**Case 9**
Present age (yr)	3	1	15	10	2	3	6	14	6
Sex	Male	Female	Male	Male	Male	Female	Male	Female	Male
Mutation[b]									
cDNA	c.221_236del	c.214_217del GCACinsCA	c.562G>T	c.562G>T	Whole gene deletion	c.402_403insC	c.674A>G	c.674A>G	c.405_406insCT
Protein	p.K74fsX103	p.A72fsX86	p.G188X	p.G188X	Absent	p. S135fsX136	p.N225S	p.N225S	p.S136fsX178
Function	Severe LOF	Severe LOF	Mild LOF	Mild LOF	Absent	Severe LOF	DN	DN	Severe LOF
Ocular malformation									
Right	AO	MO	MO	MO	MO	AO	N.D.	N.D.	AO
Left	MO	MO	MO	MO	AO	AO	N.D.	N.D.	AO
Developmental delay	+	Uncertain	+	+	+	+	N.D.	N.D.	+
Prenatal growth failure[c]	−	−	−	−	−	−	N.D.	N.D.	−
Birth length (cm) (SDS)	46.5 (−1.2)	48.3 (±0)	50 (+0.5)	49 (±0)	47.9 (−0.5)	50 (+0.6)	N.D.	N.D.	49.5 (+0.2)
Birth weight (kg) (SDS)	2.77 (−0.5)	3.22 (+0.6)	3.62 (+1.5)	3.23 (+0.5)	2.96 (−0.1)	3.16 (+0.2)	N.D.	N.D.	3.49 (+1.2)
Birth OFC (cm) (SDS)	32.5 (−0.7)	34 (+0.7)	N.E.	32.5 (−0.7)	31.5 (−1.4)	33.7 (+0.6)	N.D.	N.D.	N.D.
Postnatal growth failure[c]	+	−	+	−	+	+	+	+	+
Present height (cm) (SDS)	76.9 (−3.3)[d]	73.2 (±0)	114.0 (−4.1)[e]	130.8 (−1.5)	78.1 (−2.4)	85.0 (−3.3)	N.D.	N.D.	81.8 (−5.3)[f]
Present weight (kg) (SDS)	8.9 (−2.6)[d]	8.3 (−0.4)	16.8 (−2.4)[e]	23.2 (−1.6)	9.9 (−1.4)	10.1 (−2.6)	N.D.	N.D.	10.7 (−2.5)[f]
Present OFC (cm) (SDS)	N.E.	N.E.	N.E.	N.E.	N.E.	46 (−1.9)	N.D.	N.D.	47.2 (−2.7)[f]
Paternal height (cm) (SDS)[c]	160 (−1.9)	168 (−0.5)	178 (+1.2)	167 (−0.7)	163 (−1.3)	170 (±0)	178 (+0.3)	188 (+1.8)	N.D.
Maternal height (cm) (SDS)[c]	150 (−1.6)	151 (−1.3)	166 (+1.5)	165 (+1.4)	170 (+2.2)	155 (−0.6)	158 (−0.8)	168 (+0.7)	N.D.
Affected pituitary hormones	GH	No	GH, TSH, PRL, LH, FSH	No	GH	GH	GH, TSH, ACTH, LH, FSH	GH, TSH, ACTH, LH, FSH	GH, TSH, ACTH, LH, FSH
MRI findings									
Pituitary hypoplasia	+	N.E.	+	N.E.	+	−	+	+	+
EPP	+	N.E.	+	N.E.	−	−	+	−	+
Other features	Retractile testis (R)			Seizure		Cleft palate			Chiari malformation

SDS, SD score; OFC, occipitofrontal head circumference; MRI, magnetic resonance imaging; LOF, loss of function; DN, dominant negative; AO, anophthalmia; MO, microphthalmia; N.D., not described; N.E., not examined; PRL, prolactin; R, right.

[a] Case 6, Dateki *et al.* (8); cases 7 and 8, Diaczok *et al.* (9); case 9, Tajima *et al.* (10); [b] the cDNA and protein numbes are based on the human *OTX2* isoform-b (GenBank accession no. NM_172337.1), and the A of the ATG encoding the initiator methionine residue is denoted position +1; thus, the description of the mutations in cases 7–9 is different from that reported by Diaczok *et al.* (9) and Tajima *et al.* (10); [c] assessed by the age- and sex-matched Japanese growth standards (27) (cases 1–6 and 9 and their parents) or by the American growth standards (28) (the parents of cases 7 and 8); [d] at 2 yr 4 months of age before GH treatment; [e] at 10 yr of age before GH treatment; [f] at 4 yr of age before GH treatment.

TABLE 2. Blood hormone values in cases 1–5 with heterozygous *OTX2* mutations

Patient Sex (age at examination)		Case 1 Male (2 yr)		Case 2 Female (1 yr)		Case 3 Male (14 yr)		Case 4 Male (10 yr)		Case 5 Male (2 yr)	
	Stimulus (dose)	Basal	Peak	Basal	Peak	Basal	Peak	Basal	Peak	Basal	Peak
GH (ng/ml)	Insulin (0.1 U/kg)[a]	1.9[b]	**4.0**[b]	3.3[b]	N.E.	0.8[b]	**1.3**[b]	12.1[b]	N.E.	0.5[c]	**9.0**[c]
	Arginine (0.5 g/kg)									1.1[c]	**7.0**[c]
	L-dopa (10 mg/kg)	1.5[b]	**3.8**[b]			0.3[b]	**1.0**[b]				
LH (mIU/ml)	GnRH (100 μg/m^2)	0.1	1.7	0.1	N.E.	2.3[d]	**4.5**	0.4	N.E.	0.1	3.1
FSH (mIU/ml)	GnRH (100 μg/m^2)	1.0	6.2	3.7	N.E.	1.3[d]	**6.3**	1.1	N.E.	1.5	9.9
TSH (μU/ml)	TRH (10 μg/kg)	4.2	23.8	1.1	N.E.	0.2	**1.9**	1.1	N.E.	5.2	19.5
Prolactin (ng/ml)	TRH (10 μg/kg)	17.9	34.5	N.E.	N.E.	5.5	**8.3**	9.1	N.E.	10.43	88.8
ACTH (pg/ml)	Insulin (0.1 U/kg)	31	195	N.E.	N.E.	24		N.E.	N.E.	41	222
Cortisol (μg/dl)[d]	Insulin (0.1 U/kg)	12.7		9.4	N.E.	19.4		N.E.	N.E.	25.4	39.2
IGF-I (ng/ml)		**8**		65	N.E.	**5**		214	N.E.	48	
Testosterone (ng/dl)		N.E.		N.E.	N.E.	**45**		<5	N.E.	N.E.	
Free T_4 (ng/dl)		1.32		1.17	N.E.	**0.87**		1.15	N.E.	1.17	
Free T_3 (pg/ml)		2.91		3.24	N.E.	**1.94**		3.92	N.E.	4.54	

The conversion factor to the SI unit: GH, 1.0 (μg/liter); LH, 1.0 (IU/liter); FSH, 1.0 (IU/liter); TSH, 1.0 (mIU/liter); prolactin, 1.0 (μg /liter); ACTH, 0.22 (pmol/liter); cortisol, 27.59 (nmol/liter); IGF-I, 0.131 (nmol/liter); testosterone, 0.035 (nmol/liter); free T_4, 12.87 (pmol/liter); and free T_3, 1.54 (pmol/liter). Hormone values have been evaluated by the age- and sex-matched Japanese reference data (29, 30); low hormone data are *boldfaced*. Blood sampling during the provocation tests: 0, 30, 60, 90, and 120 min. N.E., Not examined.

[a] Sufficient hypoglycemic stimulations were obtained during all the insulin provocation tests; [b] GH was measured using the recombinant GH standard, and the peak GH values of 6 and 3 ng/ml are used as the cutoff values for partial and severe GH deficiency, respectively; [c] GH was measured by the classic RIA, and the peak GH values of 10 and 5 ng/ml were used as the cutoff values for partial and severe GH deficiency; [d] Obtained at 0800–0900 h.

gests that the biological functions of *OTX2* are primarily contributed by the short isoform-b.

Clinical features of cases 1–5 are summarized in Table 1, together with those of the previously reported *OTX2* mutation-positive patients examined for detailed pituitary function. Here four patients with cytogenetically recognizable deletions involving *OTX2* are not included (19–22) because the deletions appear to have removed a large number of genes including *BMP4* and/or *SIX6* (Fig. 2B) that can be relevant to pituitary development and/or function (1, 23).

Several points are noteworthy for the clinical findings. First, although cases 1–5 in this study had anophthalmia and/or microphthalmia, ocular phenotype has not been described in cases 7 and 8 identified by *OTX2* mutation analysis in 50 patients with hypopituitarism (9). Whereas no description of a phenotype would not necessarily indicate the lack of the phenotype, *OTX2* mutations may specifically affect pituitary function at least in several patients. This would not be unexpected because several *OTX2* mutation-positive patients are free from ocular anomalies (6).

Second, pituitary phenotype is variable and independent of the *in vitro* function data. This would be explained by the notion that haploinsufficiency of developmental genes is usually associated with a wide range of penetrance and expressivity depending on other genetic and environmental factors (24), although the actual underlying factors remain to be identified. In this regard, because direct mRNA analysis was not performed, it might be possible that the mutations have not produced the predicted aberrant protein and, consequently, *in vitro* function data do not necessarily reflect the *in vivo* functions. Even if this is the case, the quite different pituitary phenotype between cases 3 and 4 with the same mutation would argue for the notion that pituitary phenotype is independent of the residual OTX2 function.

Third, cases 1, 3, 5, and 6–9 with pituitary dysfunction have IGHD or CPHD involving GH, and show the combination of preserved prenatal growth and compromised postnatal growth characteristic of GH deficiency (25). This suggests that GH is the most vulnerable pituitary hormone in *OTX2* mutations. Consistent with this, previously reported patients with ocular anomalies and *OTX2* mutations also frequently exhibit short stature (6, 8). Thus, pituitary function studies are recommended in patients with ocular anomalies and postnatal short stature to allow for appropriate hormone therapies including GH treatment for short stature, cortisol supplementation at a stress period, T_4 supplementation to protect the developmental deterioration, and sex steroid supplementation to induce secondary sexual characteristics. Furthermore, *OTX2* mutation analysis is also recommended in such patients.

Lastly, PH and/or EPP is present in patients with IGHD and CPHD, except for case 6 with IGHD. In this regard, the following findings are noteworthy: 1) heterozygous loss-of-function mutations of *HESX1* are associated with a wide phenotypic spectrum including CPHD, IGHD, and apparently normal phenotype and often cause PH and

EPP, whereas homozygous *HESX1* mutations usually lead to CPHD as well as PH and EPP (2); 2) heterozygous loss-of-function mutations of *POU1F1* usually permit apparently normal pituitary phenotype, whereas homozygous loss-of-function mutations and heterozygous dominant-negative mutations usually result in GH, TSH, and prolactin deficiencies and often cause PH but not EPP (2); and 3) heterozygous *GNRH1* frameshift mutation are free from discernible phenotype, whereas homozygous *GNRH1* mutations result in isolated hypogonadotropic hypogonadism with no abnormal pituitary structure (26). Collectively, overall pituitary phenotype may primarily be ascribed to reduced *HESX1* expression, although reduced *POU1F1* and *GNRH1* expressions would also play a certain role, and there may be other target genes of *OTX2*.

In summary, the results imply that *OTX2* mutations are associated with variable pituitary phenotype, with no genotype-phenotype correlations, and that *OTX2* can transactivate *GNRH1* as well as *HESX1* and *POU1F1*. Further studies will serve to clarify the role of *OTX2* in the pituitary development and function.

Acknowledgments

We thank the patients and parents for participating in this study. We also thank Dr. Nicola Ragge and Dr. David J Bunyan for the MLPA probe sequence of *OTX2*.

Address all correspondence and requests for reprints to: Dr. T. Ogata, Department of Endocrinology and Metabolism, National Research Institute for Child Health and Development, 2-10-1 Ohkura, Setagaya, Tokyo 157-8535, Japan. E-mail: tomogata@nch.go.jp.

This work was supported by Grants-in-Aid for Young Scientists (B-21791025) from the Ministry of Education, Culture, Sports, Science, and Technology and Grants for Child Health and Development (20C-2); Research on Children and Families (H21-005); and Research on Measures for Intractable Diseases (H21-043) from the Ministry of Health, Labor, and Welfare.

Disclosure Summary: The authors have nothing to declare.

References

1. **Cohen LE, Radovick S** 2002 Molecular basis of combined pituitary hormone deficiencies. Endocr Rev 23:431–442
2. **Kelberman D, Dattani MT** 2007 Hypopituitarism oddities: congenital causes. Horm Res 68(Suppl 5):138–144
3. **Vieira TC, Boldarine VT, Abucham J** 2007 Molecular analysis of PROP1, PIT1, HESX1, LHX3, and LHX4 shows high frequency of PROP1 mutations in patients with familial forms of combined pituitary hormone deficiency. Arq Bras Endocrinol Metab 51:1097–1103
4. **Hever AM, Williamson KA, van Heyningen V** 2006 Developmental malformations of the eye: the role of *PAX6*, *SOX2* and *OTX2*. Clin Genet 69:459–470
5. **Courtois V, Chatelain G, Han ZY, Le Novère N, Brun G, Lamonerie T** 2003 New Otx2 mRNA isoforms expressed in the mouse brain. J Neurochem 84:840–853
6. **Ragge NK, Brown AG, Poloschek CM, Lorenz B, Henderson RA, Clarke MP, Russell-Eggitt I, Fielder A, Gerrelli D, Martinez-Barbera JP, Ruddle P, Hurst J, Collin JR, Salt A, Cooper ST, Thompson PJ, Sisodiya SM, Williamson KA, Fitzpatrick DR, van Heyningen V, Hanson IM** 2005 Heterozygous mutations of *OTX2* cause severe ocular malformations. Am J Hum Genet 76:1008–1022
7. **Wyatt A, Bakrania P, Bunyan DJ, Osborne RJ, Crolla JA, Salt A, Ayuso C, Newbury-Ecob R, Abou-Rayyah Y, Collin JR, Robinson D, Ragge N** 2008 Novel heterozygous OTX2 mutations and whole gene deletions in anophthalmia, microphthalmia and coloboma. Hum Mutat 29:E278–E283
8. **Dateki S, Fukami M, Sato N, Muroya K, Adachi M, Ogata T** 2008 OTX2 mutation in a patient with anophthalmia, short stature, and partial growth hormone deficiency: functional studies using the IRBP, HESX1, and POU1F1 promoters. J Clin Endocrinol Metab 93:3697–3702
9. **Diaczok D, Romero C, Zunich J, Marshall I, Radovick S** 2008 A novel dominant-negative mutation of OTX2 associated with combined pituitary hormone deficiency. J Clin Endocrinol Metab 93:4351–4359
10. **Tajima T, Ohtake A, Hoshino M, Amemiya S, Sasaki N, Ishizu K, Fujieda K** 2009 OTX2 loss of function mutation causes anophthalmia and combined pituitary hormone deficiency with a small anterior and ectopic posterior pituitary. J Clin Endocrinol Metab 94:314–319
11. **Cartegni L, Chew SL, Krainer AR** 2002 Listening to silence and understanding nonsense: exonic mutations that affect splicing. Nat Rev Genet 3:285–298
12. **Strachan T, Read AP** 2004 Instability of the human genome: mutation and DNA repair. In: Human molecular genetics. 3rd ed. London and New York: Garland Science; 334–337
13. **Holbrook JA, Neu-Yilik G, Hentze MW, Kulozik AE** 2004 Nonsense-mediated decay approaches the clinic. Nat Genet 36:801–808
14. **Schouten JP, McElgunn CJ, Waaijer R, Zwijnenburg D, Diepvens F, Pals G** 2002 Relative quantification of 40 nucleic acid sequences by multiplex ligation-dependent probe amplification. Nucleic Acids Res 30:e57
15. **Kelley CG, Lavorgna G, Clark ME, Boncinelli E, Mellon PL** 2000 The Otx2 homeoprotein regulates expression from the gonadotropin-releasing hormone proximal promoter. Mol Endocrinol 14:1246–1256
16. **Matsuo N** 1993 Skeletal and sexual maturation in Japanese children. Clin Pediatr Endocrinol 2(Suppl):1–4
17. **Chatelain G, Fossat N, Brun G, Lamonerie T** 2006 Molecular dissection reveals decreased activity and not dominant-negative effect in human OTX2 mutants. J Mol Med 84:604–615
18. **den Dunnen JT, White SJ** 2006 MLPA and MAPH: sensitive detection of deletions and duplications. Curr Protoc Hum Genet Chapter 7, Unit 7.14
19. **Bennett CP, Betts DR, Seller MJ** 1991 Deletion 14q (q22q23) associated with anophthalmia, absent pituitary, and other abnormalities. J Med Genet 28:280–281
20. **Elliott J, Maltby EL, Reynolds B** 1993 A case of deletion 14(q22.1→q22.3) associated with anophthalmia and pituitary abnormalities. J Med Genet 30:251–252
21. **Lemyre E, Lemieux N, Décarie JC, Lambert M** 1998 Del(14)(q22.1q23.2) in a patient with anophthalmia and pituitary hypoplasia. Am J Med Genet 77:162–165
22. **Nolen LD, Amor D, Haywood A, St Heaps L, Willcock C, Mihelec M, Tam P, Billson F, Grigg J, Peters G, Jamieson RV** 2006 Deletion at 14q22–23 indicates a contiguous gene syndrome comprising anophthalmia, pituitary hypoplasia, and ear anomalies. Am J Med Genet A 140:1711–1718

23. **Zhu X, Lin CR, Prefontaine GG, Tollkuhn J, Rosenfeld MG** 2005 Genetic control of pituitary development and hypopituitarism. Curr Opin Genet Dev 15:332–340
24. **Fisher E, Scambler P** 1994 Human haploinsufficiency — one for sorrow, two for joy. Nat Genet 7:5–7
25. **Parks JS, Felner EI** 2007 Hypopituitarism. In: Kliegman RM, Behrman RE, Jenson HB, Stanton BF, eds. Nelson textbook of pediatrics. 18th ed. Philadelphia: Saunders Elsevier; 2293–2299
26. **Bouligand J, Ghervan C, Tello JA, Brailly-Tabard S, Salenave S, Chanson P, Lombès M, Millar RP, Guiochon-Mantel A, Young J** 2009 Isolated familial hypogonadotropic hypogonadism and a GNRH1 mutation. N Engl J Med 360:2742–2748
27. **Suwa S, Tachibana K, Maesaka H, Tanaka T, Yokoya S** 1992 Longitudinal standards for height and height velocity for Japanese children from birth to maturity. Clin Pediatr Endocrinol 1:5–13
28. **Kuczmarski RJ, Ogden CL, Guo SS, Grummer-Strawn LM, Flegal KM, Mei Z, Wei R, Curtin LR, Roche AF, Johnson CL** 2002 2000 CDC growth charts for the United States: methods and development. Vital Health Stat 11 246:1–190
29. **Japan Public Health Association** 1996 Normal biochemical values in Japanese children (in Japanese). Tokyo: Sanko Press
30. **Inada H, Imamura T, Nakajima R** 2002 Manual of endocrine examination for children (in Japanese). Osaka: Medical Review